LETTERS

Immortalization eliminates a roadblock during cellular reprogramming into iPS cells

Jochen Utikal[1,2,3]*, Jose M. Polo[1,2]*, Matthias Stadtfeld[1,2], Nimet Maherali[1,2,4], Warakorn Kulalert[1,2], Ryan M. Walsh[1,2], Adam Khalil[1,2], James G. Rheinwald[5] & Konrad Hochedlinger[1,2]

The overexpression of defined transcription factors in somatic cells results in their reprogramming into induced pluripotent stem (iPS) cells[1–3]. The extremely low efficiency and slow kinetics of *in vitro* reprogramming suggest that further rare events are required to generate iPS cells. The nature and identity of these events, however, remain elusive. We noticed that the reprogramming potential of primary murine fibroblasts into iPS cells decreases after serial passaging and the concomitant onset of senescence. Consistent with the notion that loss of replicative potential provides a barrier for reprogramming, here we show that cells with low endogenous p19[Arf] (encoded by the *Ink4a/Arf* locus, also known as *Cdkn2a* locus) protein levels and immortal fibroblasts deficient in components of the *Arf–Trp53* pathway yield iPS cell colonies with up to threefold faster kinetics and at a significantly higher efficiency than wild-type cells, endowing almost every somatic cell with the potential to form iPS cells. Notably, the acute genetic ablation of *Trp53* (also known as *p53*) in cellular sub-populations that normally fail to reprogram rescues their ability to produce iPS cells. Our results show that the acquisition of immortality is a crucial and rate-limiting step towards the establishment of a pluripotent state in somatic cells and underscore the similarities between induced pluripotency and tumorigenesis.

The possibility to generate patient-specific pluripotent cells may enable the study and treatment of several degenerative diseases and therefore has enormous therapeutic potential. A major limitation of inducing pluripotency, however, is its low efficiency, which ranges between 0.01% and 0.2% when using direct viral infection of adult cells with vectors expressing the four reprogramming factors—Oct4 (also known as Pou5f1), Sox2, Klf4 and c-Myc[2,4–6]—and reaches up to ~5% when using optimized 'secondary systems'[7–9]. Secondary systems are based on somatic cells that already carry all four reprogramming transgenes in their genome under the control of doxycycline-inducible elements, thus enabling homogeneous factor expression (Supplementary Fig. 1). The low efficiency of reprogramming secondary cells suggests that other molecular events are required that restrict the conversion of somatic cells into iPS cells[1]. Identifying these restrictions is critical for understanding the mechanisms of induced pluripotency as well as for its potential clinical applications.

We noticed that secondary murine embryonic fibroblasts (MEFs) at early passages generate iPS cells more efficiently than MEFs at later passages, consistent with the notion that a high replicative potential of somatic cells is critical for successful reprogramming into iPS cells (Fig. 1a, top row). The accumulation of β-galactosidase-positive senescent cells in late passage cultures further suggests that molecular

changes associated with cellular senescence provide a roadblock for the conversion of somatic cells into iPS cells (Fig. 1a, bottom row). The loss of replicative potential is often the consequence of culture-induced upregulation of the cell-cycle-dependent kinase inhibitors p16[Ink4a], p19[Arf] (which are encoded by alternative reading frames of the *Ink4a/Arf* locus), p21[Cip1] (Cdkn1a), as well as activation of Trp53 (ref. 10). Indeed, we observed a progressive upregulation of *Ink4a*,
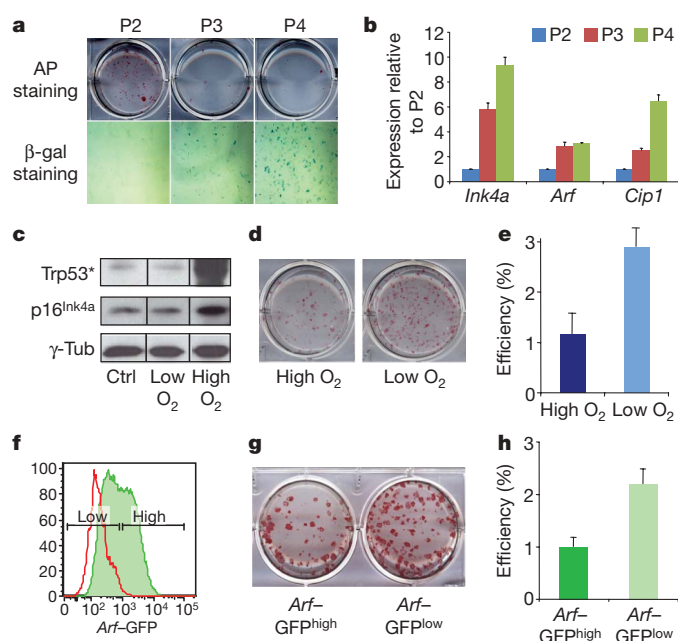

Figure 1 | Reprogramming efficiency of fibroblasts is influenced by replicative potential and *Arf* expression status. a, Alkaline phosphatase (AP) staining (top) of iPS cell colonies derived from secondary murine embryonic fibroblasts (MEFs) at different passages (P). Senescence associated β-galactosidase activity (bottom) of MEFs at the same passages. Original magnification, × 200. **b,** Expression levels of *Ink4a*, *Arf* and *Cip1* in MEFs at the same passages as shown in **a** (n = 2). **c,** Western blot analysis of p16[Ink4a] and phosphorylated-Trp53 (Trp53*) in MEFs grown at low (4%) or high (21%) oxygen for 6 days. Ctrl, control MEFs at day 1. **d, e,** Secondary MEFs grown under low O₂ give rise to iPS cells more efficiently (n = 3). **f,** *Arf*–GFP reporter MEFs (green line) at passage 3 show heterogeneous expression levels. Shown in red are wild-type MEFs. **g, h,** *Arf*–GFP[low] MEFs give rise to iPS cell colonies more efficiently than *Arf*–GFP^{high} cells (n = 2). See Methods for details on measuring efficiencies. All error bars depict the s.e.m.

[1]Massachusetts General Hospital Cancer Center and Center for Regenerative Medicine, Harvard Stem Cell Institute, 185 Cambridge Street, Boston, Massachusetts 02114, USA. [2]Department of Stem Cell and Regenerative Biology, Harvard University, Cambridge, Massachusetts 02138, USA. [3]Department of Dermatology, Venereology and Allergology, University Medical Center Mannheim, Ruprecht-Karl-University of Heidelberg, Theodor-Kutzer-Ufer 1-3, 68135 Mannheim, Germany. [4]Department of Molecular and Cellular Biology, Harvard University, 7 Divinity Avenue, Cambridge, Massachusetts 02138, USA. [5]Department of Dermatology, Brigham and Women's Hospital and Harvard Skin Disease Research Center, 77 Avenue Louis Pasteur, Boston, Massachusetts 02115, USA.
*These authors contributed equally to this work.

1145

Arf and *Cip1* transcript levels in serially passaged MEFs (Fig. 1b). Growth of MEFs in low oxygen (4%) can counteract culture-induced upregulation of p16[Ink4a], p19[Arf] and activation of Trp53, thereby extending replicative lifespan (Fig. 1c)[11]. We detected a threefold increase in reprogramming efficiency in secondary MEFs cultured in low oxygen (Fig. 1d, e), in agreement with the notion that p16[Ink4a] and activated Trp53 inhibit reprogramming.

To test directly whether the expression status of the *Ink4a/Arf* locus in the starting cell population has an influence on reprogramming, we analysed cells derived from an *Arf*–green fluorescent protein (GFP) knock-in reporter mouse[12]. *Arf*–GFP MEFs at passage 3 contained a population of *Arf*–GFP[high] and *Arf*–GFP^{low} cells, consistent with previous observations[12] (Fig. 1f). Interestingly, fluorescence-activated cell sorting (FACS)-purified *Arf*–GFP[low] MEFs yielded iPS cell colonies twice as efficiently as *Arf*–GFP[high] MEFs, indicating that reduced *Arf* levels in the starting cell population are beneficial for reprogramming (Fig. 1g, h).

Notably, *Arf*–GFP expression was undetectable and endogenous *Ink4a* and *Arf* transcript levels were downregulated in established iPS cells (Fig. 2a and Supplementary Fig. 2a), further indicating that inactivation of this key senescence pathway by the reprogramming factors may be critical for the acquisition of pluripotency. In agreement, expression of the four reprogramming factors for 6 days resulted in efficient downregulation of the *Arf*–GFP allele (Fig. 2a). However, no single reprogramming factor alone was sufficient to silence *Arf*–GFP expression (Fig. 2a), suggesting that the synergistic action of at least two of the factors is required to inhibit *Arf* transcription.

To examine how silencing of the *Ink4a/Arf* locus correlates with other markers that change during reprogramming, we followed the expression of *Arf*–GFP in intermediate cell populations previously identified by surface markers[13,14]. Notably, *Arf* expression was downregulated specifically in the Thy1^{−} and SSEA1^{+} fractions, which are enriched for cells poised to become iPS cells, but not in the Thy1^{+}

fraction, which fails to give rise to iPS cells (Fig. 2b). *Ink4a* RNA and protein levels followed a similar trend as the *Arf*–GFP expression during reprogramming (Supplementary Fig. 3). Of note, SSEA1^{+} *Arf*–GFP^{low} cells had a threefold higher reprogramming potential than SSEA1^{+} *Arf*–GFP^{high} cells, indicating that low *Arf* expression is a useful prospective marker to further enrich for intermediate cells poised to become iPS cells (Fig. 2c, d). Together, these results show that downregulation of the *Ink4a/Arf* locus correlates well with, and further refines previously identified subpopulations of cells undergoing reprogramming.

Using a published PCR-based assay[15], we found that iPS cells and ES cells, in contrast to MEFs, show *Ink4a/Arf* promoter methylation, consistent with stable transcriptional silencing of *Ink4a/Arf* in pluripotent cells (Supplementary Fig. 2b). However, the downregulation of *Arf*–GFP expression at day 6 of reprogramming as seen by FACS (Fig. 2b) was not yet accompanied by detectable promoter methylation, suggesting that stable silencing of the *Ink4a/Arf* locus is a late event during reprogramming that requires further molecular changes. In agreement with a transient decrease in *Arf* expression, the withdrawal of doxycycline from day 6 cultures resulted in the rapid re-appearance of *Arf*–GFP expression and the failure to recover stable iPS cell colonies (Fig. 2b and data not shown). Promoter methylation first became detectable at day 9 of reprogramming in the SSEA1^{+} fraction (Supplementary Fig. 2b), which contains most stably reprogrammed cells[13]. This observation indicates that the stable silencing of the *Ink4a/Arf* locus is achieved by epigenetic modifications and occurs specifically in late intermediate cells that are poised to become iPS cells.

Because genetic deletion of the entire *Ink4a/Arf* locus in fibroblasts results in their immortalization[16], we wondered whether immortalized somatic cells are more amenable to reprogramming than primary cells. We first assessed the reprogramming potential of a spontaneously immortalized melanocyte line[17] (designated 'Melan A'). Melan A cells gave rise to iPS cells four times more efficiently than primary melanocytes, yielding efficiencies close to 1% (Fig. 3a and Supplementary Fig. 4a–d). Injection of these iPS cells into severe combined immunodeficient (SCID) mice gave rise to well-differentiated teratomas, and introduction into blastocysts yielded chimaeric mice that showed contribution to different tissues (Fig. 3b, c and Supplementary Fig. 4e). These results document that an established cell line remains permissive for reprogramming into a pluripotent state. Spontaneous immortalization of cultured cells is usually accompanied by mutations of components of the *Arf*–Trp53 pathway[18]. Indeed, western blot analysis showed the absence of p16[Ink4a] protein in Melan A cells (Supplementary Fig. 4f) even though sequence analysis of the *Ink4a* and *Arf* exons did not reveal any mutations (data not shown).

To assess more accurately reprogramming frequencies of immortalized versus primary melanocytes, we established secondary cells by *in vitro* differentiation of iPS cells[7,8] (Supplementary Figs 1 and 5a). Secondary cells obtained from primary melanocytes converted into iPS cells at an average efficiency of 1.5%, consistent with previous observations[7–9,19] (Fig. 3d, clones 1–3). Remarkably, however, Melan A-derived secondary cells gave rise to iPS cells at efficiencies of up to ~65%, indicating that immortalization endows almost two in three cells with the potential to form iPS cells (Fig. 3d, clones 57–61 and Supplementary Fig. 5b). Moreover, single-cell sorting of one subclone (clone 59.3) generated iPS cells at 100% efficiency, demonstrating that most, if not all, of the cells are endowed with the potential to give rise to pluripotent colonies (Fig. 3e). Secondary MEFs obtained from Melan A-iPS cells at embryonic day (E) 14.5 gave rise to iPS cell colonies at an efficiency of ~40%, which is comparable to *in vitro*-derived secondary cells (Fig. 3d, clones M4 and M7).

We next tested whether deletion of *Trp53* or *Ink4a/Arf* in fibroblasts mimics the phenotype of spontaneously immortalized cells. Indeed, we observed a 30–40-fold increase in the number of iPS cell colonies in *Trp53*, compound *Ink4a/Arf* and single *Arf* mutant cells compared with wild-type control cells, demonstrating that inactivation of these pathways is probably responsible for the increased reprogramming efficiencies of spontaneously immortalized cells (Fig. 3f,
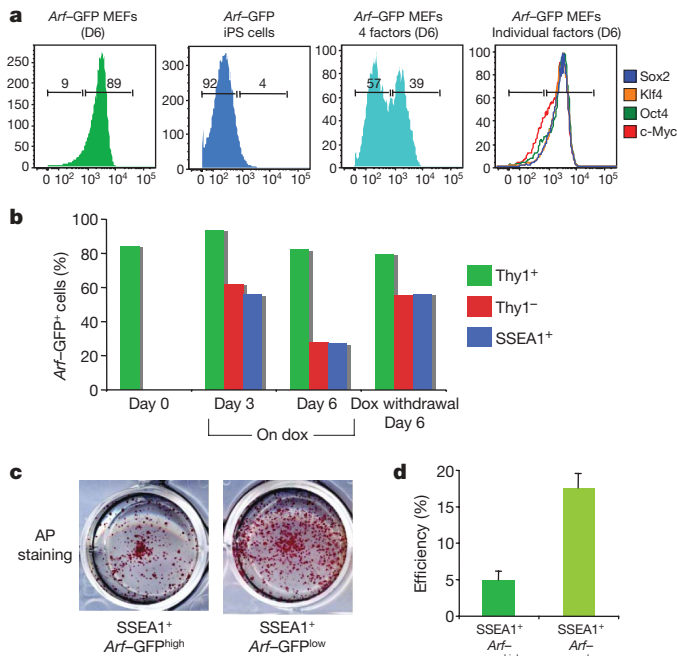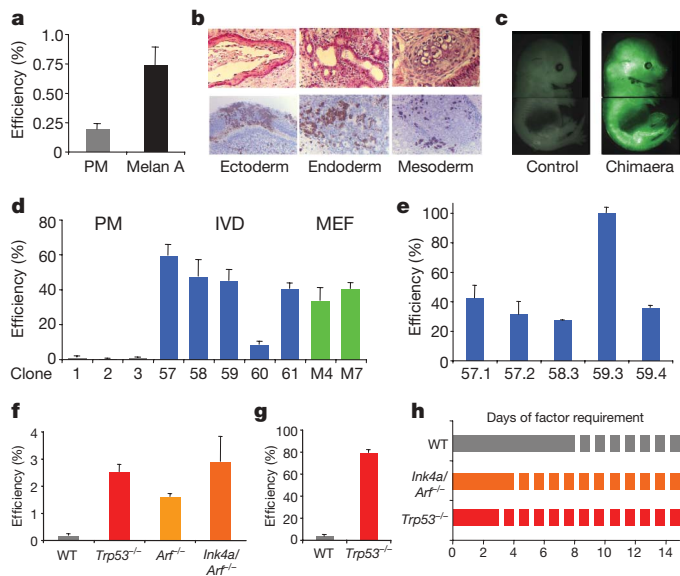

Figure 2 | Transcription-factor-induced downregulation of *Ink4a/Arf* expression in cells undergoing reprogramming. a, FACS plots of sorted *Arf*–GFP[high] MEFs (left), established iPS cells from *Arf*–GFP MEFs (left middle), *Arf*–GFP[high] MEFs expressing all four reprogramming factors (right middle) or each factor individually (right). Cells withdrawn from doxycycline (dox) on day 6 were analysed 3 days later. D6, day 6. **b**, Time course of *Arf*–GFP expression in subpopulations of cells undergoing reprogramming. **c, d**, *Arf*–GFP[low] SSEA1^{+} cells at 6 days of transgene expression give rise to more transgene-independent alkaline phosphatase (AP)[+] iPS cell colonies than *Arf*–GFP[high] SSEA1^{+} cells (*n* = 3). Error bars depict the s.e.m.

Figure 3 | Cellular immortalization enhances reprogramming potential and kinetics. a, The spontaneously immortalized Melan A cell line yields iPS colonies 3–4 times more efficiently than primary melanocytes (PM) after direct viral infection ($n = 3$). **b, c**, Melan A-derived iPS cells show differentiation into ectodermal, mesodermal and endodermal derivatives in teratomas (**b**, top) and in chimaeras produced from iPS cells labelled with a lentivirus constitutively expressing GFP (**b**, bottom, and **c**). Original magnification, ×400. **d**, iPS cell formation efficiency of secondary cells derived from primary melanocytes (grey bars), Melan A-derived *in vitro*-differentiated (IVD) cells (blue bars) or Melan A-derived MEFs (green bars) ($n = 3$). **e**, iPS cell formation efficiency of subclones of Melan A-derived IVD secondary cells ($n = 3$). **f**, Reprogramming efficiency of wild-type (WT), $Trp53^{-/-}$, $Arf^{-/-}$ and $Ink4a/Arf^{-/-}$ MEFs after direct viral infection ($n = 3$). **g**, Reprogramming potential of secondary $Trp53^{-/-}$ iPS cell-derived E14.5 MEFs ($n = 2$). **h**, Evaluation of minimal temporal transgene requirement (solid lines) in wild-type, $Ink4a/Arf^{-/-}$ and $Trp53^{-/-}$ MEFs to form stable iPS cell colonies. All error bars depict s.e.m.

Supplementary Fig. 6 and Supplementary Table 1). Moreover, $Trp53^{-/-}$ iPS-cell-derived E14.5 secondary MEFs gave rise to iPS cell colonies at an efficiency of ~80%, similar to results obtained with spontaneously immortalized cells (Fig. 3g). Collectively, these observations provide strong functional evidence that the inactivation of key pathways controlling replicative potential and senescence substantially enhance the reprogramming potential of somatic cells into iPS cells.

To exclude the possibility that an altered growth rate of immortal cells rather than their long-term proliferation potential influences their increased reprogramming potential, we compared the iPS cell formation efficiencies of $Trp53^{-/-}$ and wild-type MEFs grown under low (0.5% FBS) and high (15% FBS) serum conditions. $Trp53$-deficient MEFs cultured in low serum exhibited a significantly reduced growth rate compared with MEFs cultured in high serum (Supplementary Fig. 7a). Despite this growth disadvantage, $Trp53$-mutant cells gave rise to iPS cells more efficiently than wild-type MEFs, suggesting that the long-term proliferation potential of immortal cells is responsible for their enhanced reprogramming potential (Supplementary Fig. 7b, c).

Given that the acquisition of immortality by downregulation of *Arf* or *Trp53* seems to eliminate a roadblock during the reprogramming of somatic cells into iPS cells, inactivation of these pathways might also affect the kinetics of reprogramming. Indeed, although wild-type cells required 8 days of transgene expression to produce stable iPS cells, which is consistent with a previous report[13], $Trp53$ and $Ink4a/Arf$ mutant cells gave rise to iPS cell colonies after only 3 and 4 days of transgene expression, respectively, demonstrating that the acquisition of cellular immortality is not only an efficiency-limiting but also a rate-limiting step during induced pluripotency (Fig. 3h).

Surprisingly, we failed to detect a correlation between the relative numbers of Thy1⁻ and SSEA1⁺ intermediate cells and

reprogramming efficiency in $Trp53^{-/-}$ compared with wild-type cultures (Supplementary Fig. 8). This suggests that immortal cells undergoing reprogramming pass through the same roadblocks as control cells but that immortality endows those cells that otherwise fail to reprogram with the potential to form iPS cells. To test this hypothesis further, we plated FACS-purified Thy1⁺, Thy1⁻ and SSEA1⁺ cells isolated from wild-type or $Trp53$-deficient secondary cells on feeders in the presence or absence of doxycycline (Fig. 4a). In wild-type cells, iPS cells appeared predominantly from the SSEA1⁺ population at all time points and to a lesser degree from the Thy1⁻ and Thy1⁺ fractions in the continuous presence of doxycycline (Fig. 4a, left). However, when doxycycline was withdrawn after the sorting of these populations, only the SSEA1⁺ fraction at day 9 gave rise to stable iPS cells, consistent with previous observations[13,14] (Fig. 4a, right). This result is in accordance with the earlier finding that the methylation of the $Ink4a/Arf$ locus becomes detectable specifically in the SSEA1⁺ population in wild-type cells (Supplementary Fig. 2b). In contrast, $Trp53$-deficient secondary cells continuously treated with doxycycline gave rise to iPS cells at high efficiency and regardless of the Thy1 and SSEA1 expression status (Fig. 4a, left). Moreover, when doxycycline treatment was discontinued after sorting, iPS cell colonies emerged from Thy1⁺, Thy1⁻ and SSEA1⁺
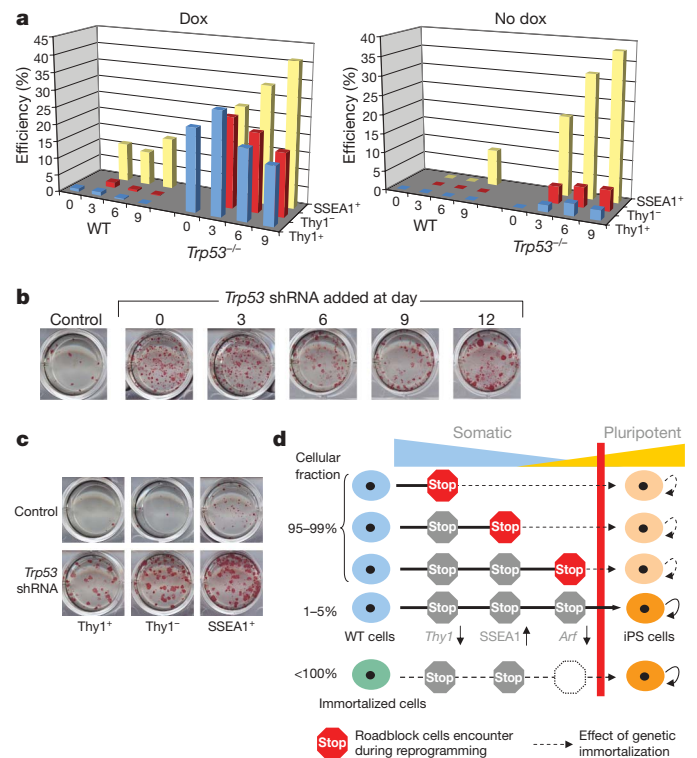

Figure 4 | $Trp53$ deficiency rescues reprogramming potential in cells that normally fail to form iPS cells. a, Comparison of reprogramming potentials of sorted Thy1⁺, Thy1⁻ and SSEA1⁺ subpopulations in wild-type and $Trp53^{-/-}$ cells at different time points (in days) during reprogramming in the presence or absence of doxycycline (dox). **b**, Acute inactivation of $Trp53$ by lentivirus expressing $Trp53$ shRNA in secondary cells increases reprogramming efficiency at all time points. **c**, Knockdown of $Trp53$ by $Trp53$ shRNA rescues the potential of Thy1⁻ and Thy1⁺ subpopulations to generate iPS cells. **d**, Model summarizing the presented data. During factor-induced reprogramming, cells encounter different roadblocks, such as the successful silencing of somatic genes (for example, *Thy1*), the activation of pluripotency genes (for example, SSEA1) and eventually the acquisition of immortality (for example, silencing of *Arf*). The low efficiency of the process is probably due to the capacity of rare cells to overcome these roadblocks. In immortal fibroblasts, however, almost every cell is endowed with the potential to produce iPS cells. Moreover, cells that have already encountered a roadblock can be rescued by acute inactivation of $Trp53$ (indicated by dashed black lines). Red bar illustrates the transition point between the somatic (blue) and the pluripotent (yellow) state.

cells as early as 3 days after induction of transgenes. These findings confirm that reprogramming kinetics are up to three times faster in immortal cells than primary cells, and demonstrate that *Trp53* deficiency confers reprogramming potential to cells that normally fail to form iPS cells.

Because continuous *Trp53* deficiency in MEFs may select for genomic aberrations that favour reprogramming into iPS cells, we acutely inhibited *Trp53* expression by infecting secondary wild-type cells with a lentiviral construct expressing a short hairpin RNA (shRNA) against *Trp53* (*Trp53* shRNA)[20]. We found that MEFs treated with *Trp53* shRNA at any time point during reprogramming gave rise to iPS cell colonies at higher efficiency than control cells (Fig. 4b). Furthermore, infection of Thy1^{+} and Thy1^{−} cells with *Trp53* shRNA yielded iPS cells at similar efficiencies as the SSEA1^{+} population, demonstrating that the acute inactivation of Trp53 is sufficient to confer the ability to undergo reprogramming on cells that would otherwise fail to form iPS cells (Fig. 4c). Likewise, the treatment of senescent cultures, which appear refractory to reprogramming, with *Trp53* shRNA rescued their ability to produce iPS cells (Supplementary Fig. 9). Notably, we demonstrate a continuous requirement for the absence of Trp53 to elicit an enhanced effect on reprogramming using a Cre-reactivatable allele of *Trp53* (Supplementary Fig. 10).

Furthermore, we sought to determine whether human immortalized cells are equally amenable to reprogramming as murine cells. To this end, we compared the reprograming abilities of primary and TERT-immortalized human keratinocyte cell lines, which show comparable growth rates but obvious differences in their long-term proliferation potential[21]. Indeed, TERT-immortalized keratinocyte lines gave rise to iPS-cell-like colonies ~20 times more efficiently than early passage cultures of the primary keratinocyte line, from which they were derived (strain N)[21], indicating that overcoming replicative senescence may be critical during the reprogramming of both murine and human somatic cells into iPS cells (Supplementary Fig. 11).

Our results indicate that the acquisition of immortality by epigenetic silencing of the *Ink4a/Arf* locus provides a bottleneck for the conversion of somatic cells into iPS cells, thus contributing to the low efficiency and delayed kinetics of *in vitro* reprogramming. After immortalization of fibroblasts, however, almost every somatic cell (or its clonal offspring) is endowed with the potential to generate iPS cells (Fig. 4d). Our findings are consistent with previous reports showing a more subtle effect of genetically interfering with immortalization pathways on iPS cell formation efficiency in human cells[22,23]. Because Trp53 and p19[Arf] are guardians of chromosomal stability, however, their manipulation in a therapeutic setting should be approached with caution. Primary cell populations with low endogenous levels of active Trp53 or p16[Ink4a] and p19[Arf] (refs 24–26) or cells with a high endogenous proliferative potential, such as somatic stem and progenitor cells[27], might provide an alternative and safer source for producing iPS cells at high efficiency.

METHODS SUMMARY

To generate iPS cells, primary and immortalized cell populations were infected with lentiviral vectors expressing Oct4, Sox2, Klf4 and c-Myc from a polycistronic construct under the control of a doxycycline-inducible promoter, together with a lentivirus constitutively expressing the M2 reverse tetracycline transactivator (M2-rtTA). Secondary cells were derived either by *in vitro* differentiation of iPS cells or after blastocyst injection and isolation of fibroblasts from chimaeras. The developmental potential of iPS cells was assessed by teratoma formation after subcutaneous injection into immunocompromised mice and by chimaera formation after blastocyst injection. Intermediate cell populations were isolated by flow cytometry.

Full Methods and any associated references are available in the online version of the paper at www.nature.com/nature.

1. Hochedlinger, K. & Plath, K. Epigenetic reprogramming and induced pluripotency. *Development* **136**, 509–523 (2009).
2. Takahashi, K. *et al.* Induction of pluripotent stem cells from adult human fibroblasts by defined factors. *Cell* **131**, 861–872 (2007).
3. Takahashi, K. & Yamanaka, S. Induction of pluripotent stem cells from mouse embryonic and adult fibroblast cultures by defined factors. *Cell* **126**, 663–676 (2006).
4. Maherali, N. *et al.* Directly reprogrammed fibroblasts show global epigenetic remodeling and widespread tissue contribution. *Cell Stem Cell* **1**, 55–70 (2007).
5. Okita, K., Ichisaka, T. & Yamanaka, S. Generation of germline-competent induced pluripotent stem cells. *Nature* **448**, 313–317 (2007).
6. Wernig, M. *et al.* *In vitro* reprogramming of fibroblasts into a pluripotent ES-cell-like state. *Nature* **448**, 318–324 (2007).
7. Hockemeyer, D. *et al.* A drug-inducible system for direct reprogramming of human somatic cells to pluripotency. *Cell Stem Cell* **3**, 346–353 (2008).
8. Maherali, N. *et al.* A high-efficiency system for the generation and study of human induced pluripotent stem cells. *Cell Stem Cell* **3**, 340–345 (2008).
9. Wernig, M. *et al.* A drug-inducible transgenic system for direct reprogramming of multiple somatic cell types. *Nature Biotechnol.* **26**, 916–924 (2008).
10. Collado, M., Blasco, M. A. & Serrano, M. Cellular senescence in cancer and aging. *Cell* **130**, 223–233 (2007).
11. Parrinello, S. *et al.* Oxygen sensitivity severely limits the replicative lifespan of murine fibroblasts. *Nature Cell Biol.* **5**, 741–747 (2003).
12. Zindy, F. *et al.* Arf tumor suppressor promoter monitors latent oncogenic signals *in vivo*. *Proc. Natl Acad. Sci. USA* **100**, 15930–15935 (2003).
13. Stadtfeld, M., Maherali, N., Breault, D. T. & Hochedlinger, K. Defining molecular cornerstones during fibroblast to iPS cell reprogramming in mouse. *Cell Stem Cell* **2**, 230–240 (2008).
14. Brambrink, T. *et al.* Sequential expression of pluripotency markers during direct reprogramming of mouse somatic cells. *Cell Stem Cell* **2**, 151–159 (2008).
15. Sharpless, N. E. *et al.* Loss of p16Ink4a with retention of p19Arf predisposes mice to tumorigenesis. *Nature* **413**, 86–91 (2001).
16. Serrano, M. *et al.* Role of the INK4a locus in tumor suppression and cell mortality. *Cell* **85**, 27–37 (1996).
17. Bennett, D. C., Cooper, P. J. & Hart, I. R. A line of non-tumorigenic mouse melanocytes, syngeneic with the B16 melanoma and requiring a tumour promoter for growth. *Int. J. Cancer* **39**, 414–418 (1987).
18. Kamijo, T. *et al.* Tumor suppression at the mouse INK4a locus mediated by the alternative reading frame product p19ARF. *Cell* **91**, 649–659 (1997).
19. Hanna, J. *et al.* Direct reprogramming of terminally differentiated mature B lymphocytes to pluripotency. *Cell* **133**, 250–264 (2008).
20. Ventura, A. *et al.* Cre-lox-regulated conditional RNA interference from transgenes. *Proc. Natl Acad. Sci. USA* **101**, 10380–10385 (2004).
21. Dickson, M. A. *et al.* Human keratinocytes that express hTERT and also bypass a p16(INK4a)-enforced mechanism that limits life span become immortal yet retain normal growth and differentiation characteristics. *Mol. Cell. Biol.* **20**, 1436–1447 (2000).
22. Mali, P. *et al.* Improved efficiency and pace of generating induced pluripotent stem cells from human adult and fetal fibroblasts. *Stem Cells* **26**, 1998–2005 (2008).
23. Zhao, Y. *et al.* Two supporting factors greatly improve the efficiency of human iPSC generation. *Cell Stem Cell* **3**, 475–479 (2008).
24. Molofsky, A. V. *et al.* Increasing p16INK4a expression decreases forebrain progenitors and neurogenesis during ageing. *Nature* **443**, 448–452 (2006).
25. Krishnamurthy, J. *et al.* p16INK4a induces an age-dependent decline in islet regenerative potential. *Nature* **443**, 453–457 (2006).
26. Janzen, V. *et al.* Stem-cell ageing modified by the cyclin-dependent kinase inhibitor p16INK4a. *Nature* **443**, 421–426 (2006).
27. Eminli, S. *et al.* Differentiation stage determines reprogramming potential of hematopoietic cells into iPS cells. *Nature Genet.* (in the press).

Supplementary Information is linked to the online version of the paper at www.nature.com/nature.

Author Contributions J.U., J.M.P. and K.H. conceived the study, interpreted results and wrote the manuscript, J.U. and J.M.P. performed most of the experiments with help from W.K., R.M.W. and A.K. M.S., N.M. and J.G.R. provided essential study material and helped with interpretation of results.

Author Information Reprints and permissions information is available at www.nature.com/reprints. Correspondence and requests for materials should be addressed to K.H. (khochedlinger@helix.mgh.harvard.edu).

METHODS

Viral vectors and production. The generation and structure of replication-defective doxycycline-inducible lentiviral vectors and a lentiviral vector constitutively expressing the reverse tetracycline-controlled transactivator (rtTA) has been described in detail elsewhere[13,28]. Viral supernatant was concentrated approximately 100-fold by ultracentrifugation at 50,000g for 1.5 h at 4 °C, resuspended in 300 μl PBS, and stored at −80 °C. Infections were carried out in 1 ml medium using 5 μl of each viral concentrate per 35-mm plate. Downregulation of Trp53 expression was performed by infecting cells with a lentiviral construct expressing an shRNA against *Trp53* (GTACTCTCCTCC CCTCAAT) as previously described[20].

Cell culture and *in vitro* differentiation of iPS cells. Melan A cells were grown in RPMI medium containing 10% FCS and 200 nM 12-*O*-tetradecanoylphorbol-13-acetate (TPA)[17]. Melan A cells were single-cell cloned and only one subclone was used for subsequent experiments. Fibroblast cultures containing a reactivatable *Trp53* allele as well as the ROSA26-CreER allele[29] were obtained from the tail of an adult mouse as described previously[13]. *Trp53*$^{−/−}$ fibroblasts and *Ink4a/ Arf*$^{−/−}$ MEFs were cultured in DMEM containing 10% FCS. Primary melanocytes were purchased from the Skin Diseases Research Center, Yale School of Medicine, and were grown like Melan A cells. For lentiviral vector infections, cells were seeded in 6-well plates at a density of 1×10^5 cells per well and infected on three consecutive days. Medium changes were performed 12–24 h after infection. One day after the last infection, ES cell medium containing 1 μg ml$^{−1}$ doxycycline was added. Fresh ES cell medium with doxycycline was added every other day until iPS cell colonies developed. Five days later, cell culture conditions were switched to ES cell medium in the absence of doxycycline. iPS cell colonies were picked into 96-well plates containing PBS without magnesium and calcium using a 10-μl pipette. Trypsin was added to each well, incubated for 5 min and single-cell suspension was transferred into 24-well dishes containing MEF feeder layers. Picked iPS cells were grown on MEFs in standard ES cell conditions. For blastocyst injections, iPS cells were marked with a FUGW lentiviral vector constitutively expressing GFP. For *in vitro* differentiation assays, iPS cells were grown in the absence of leukaemia inhibitory factor (LIF) on uncoated plates to induce embryoid body formation. Embryoid bodies were explanted on gelatinized plates and outgrowths were dissociated by trypsinization and expanded for FACS purification (see flow cytometry).

Human cell culture and generation of human iPS cells. The human epidermal keratinocyte lines strain N, N/TERT-1, and N/TERT-2G were grown in keratinocyte serum-free medium (KSFM) medium as previously described[21]. STEMCCA lentiviral vector[28] infections were carried out with human keratinocytes in 6-well plates at a density of 100,000 cells per well on two subsequent days. The infection efficiency of primary human keratinocytes after two subsequent infections with tetO-GFP lentiviral vector in the presence of the rtTA expressing lentiviral vector was 40%. Medium changes were performed 12 h after infections, and 1 day after infection human keratinocytes were transferred to MEFs. Media containing 50% keratinocyte medium and 50% human ES cell medium containing 0.5 μg ml$^{−1}$ doxycycline was added 1 day later. Medium changes were performed every other day in the presence of 0.5 μg ml$^{−1}$ doxycycline until colonies developed. After the appearance of human ES-cell-like colonies, medium was switched to human ES cell culture conditions and human iPS cells were picked and further expanded as described previously[8].

Calculation of reprogramming efficiencies. For cells directly infected with lentivirus (LV-tetO-Oct4, -Sox2, -Klf4 and -c-Myc[13] plus FUGW-rtTA[13], or LV-tetO-STEMCCA[28] plus FUGW-rtTA), reprogramming efficiencies were calculated on the basis of the infection efficiency of somatic cells with a single control virus expressing EGFP (FUGW-GFP) or by performing immunofluorescence staining for Oct4 and Sox2. For secondary cells, equal numbers of cells were plated in the absence or presence of doxycycline on 100-mm dishes coated with gelatin or containing a layer of irradiated MEF feeders. Efficiencies were determined on average 20 days later by dividing the number of iPS cell colonies that grew after the withdrawal of doxycycline by the number of seeded cells, or alternatively, by the number of colonies that adhered to the control plate in the absence of doxycycline. ES cell character of iPS cell colonies was validated by immunofluorescence staining for Nanog. For some experiments, we FACS-sorted single secondary cells (previously marked with a lentiviral vector expressing td-Tomato) into wells of a 96-well plate. Reprograming was induced by treatment of cells with doxycycline for 15 days, followed by doxycycline-independent growth for another 7 days. The number of wells with ES cell-like transgene-independent colonies was then scored by morphology and alkaline phosphatase staining; ES cell phenotype of these colonies was further verified by immunofluorescence staining for Nanog and Sox2. Efficiencies were calculated

on the basis of the number of wells containing colonies, normalized by the seeding efficiency, which was determined at day 3 by the presence of at least one td-Tomato cell in the well.

Alkaline phosphatase staining. Alkaline phosphatase staining was performed using an Alkaline Phosphatase substrate kit (Vector laboratories) according to manufacturer's recommendations.

Immunofluorescence. iPS cells were cultured on pretreated coverslips, fixed with 4% PFA, and permeabilized with 0.5% Triton X-100. The cells were then stained with primary antibodies against mouse Oct4 (sc-8628, Santa Cruz), mouse Sox2 (AB5603, Chemicon), and mouse Nanog (ab21603, Abcam). Respective secondary antibodies were conjugated to Alexa Fluor 546 (Invitrogen). Nuclei were counterstained with 4,6-diamidino-2-phenylindole (DAPI; Invitrogen). Cells were imaged with a Leica DMI4000B inverted fluorescence microscope equipped with a Leica DFC350FX camera. Images were processed and analysed with Adobe Photoshop software.

Flow cytometry. Collected cells were incubated with antibodies against Thy1.2 (phycoerythrin (PE)-conjugated, 53-2.1, eBiosciences), SSEA1 (mouse IgM, MC-480, Developmental Hybridoma Bank) and Flk1 (biotinylated, Aves 12a1, eBiosciences) for 20 min. Cells were washed in PBS and then incubated for 20 min with allophycocyanin (APC)-conjugated anti mouse IgM (eBioscience) and Pacific Blue-conjugated streptavidin (Invitrogen). The cells were washed in PBS, resuspended in propidium iodide 5% FBS/PBS solution, and passed through a 40-μm cell strainer to achieve single-cell suspension. Cells positive for Thy1 and Flk1 and negative for SSEA1 were sorted on a FACSAria (BD Biosciences). For analysis and/or sorting of intermediates, cells were stained with Thy1.2 and SSEA1 antibodies and sorted or analysed as indicated.

PCR analysis. For quantitative PCR (qPCR) analysis, RNA was isolated from cells with TRIzol reagent (Invitrogen). For strongly pigmented cells, an extra phenol–chloroform purification step was performed before RNA clean up with the RNeasy Minikit (Qiagen). Complementary DNA was produced with the Super Script III kit (Invitrogen). Real-time quantitative PCR reactions were set up in triplicate with the Brilliant II SYBR Green QPCR Master Mix (Stratagene), and run on a Mx3000P QPCR System (Stratagene). Primer sequences are listed in Supplementary Table 2. Genotyping for the *Trp53*$^{−/−}$* allele was performed by PCR using the following three primer pairs: P53K_A: 5′-CAAACTGTTCTACCTCAAGAGCC-3′, P53K_B: 5′-AGCTAGCCACCATG GCTTGAGTAAGTCTGCA-3′, and P53K_C: 5′-CTTGGAGACATAGCCACA CTG-3′ (provided by A. Ventura).

Western blot analysis. Cell extracts were run in 15% SDS–PAGE gels. The gels were run at 90 V until proteins were separated (~2 h) and transferred to PVDF membranes (Bio-Rad) by running overnight at 20 V, 4 °C in transfer apparatus (Bio-Rad). The membranes were washed in PBS-T (PBS + 0.1% Tween) and blocked in 5% milk in PBS-T for 1 h. The membranes were then incubated with anti-p16^{Ink4A}, anti-Trp53 (phospho s15) (abcam) and γ-tubulin antibody overnight at 4 °C, washed and incubated in horseradish-peroxidase-conjugated anti-rabbit antibodies for 1 h at room temperature. Immunoblots were visualized using ECL reagent (Santa Cruz).

Cellular senescence detection. Cellular senescence was detected using a cellular senescence detection kit (Millipore) on the basis of β-galactosidase staining according to manufacturer's recommendations.

Bisulphite sequencing. Bisulphite treatment of DNA was performed with the EpiTect Bisulfite Kit (Qiagen) according to manufacturer's instructions. Primer sequences were as previously described for *Oct4* and *Nanog*[4]. Amplified products were purified by using gel filtration columns, cloned into the pCR4-TOPO vector (Invitrogen), and sequenced with M13 forward and reverse primers.

Generation of teratomas and chimaeras. For teratoma induction, 2×10^6 cells of each iPS cell line were injected subcutaneously into the dorsal flank of isoflurane-anaesthetized SCID mice. Teratomas were recovered 3–5 weeks after injection, fixed overnight in 10% formalin, paraffin embedded, and processed with haematoxylin and eosin. For chimaera production, female BDF1 mice were superovulated with PMS (pregnant mare serum) and hCG (human chorion gonadotropin) and mated to BDF1 stud males. Zygotes were isolated from plugged females 24 h after hCG injection. After 3 days of *in vitro* culture in KSOM media, blastocysts were injected with iPS cells, and transferred into day 2.5 pseudopregnant recipient females. Caesarean sections were performed 17 days later and pups were fostered with lactating females.

28. Sommer, C. A. *et al.* iPS cell generation using a single lentiviral stem cell cassette. *Stem Cells* **27**, 543–549 (2008).
29. Ventura, A. *et al.* Restoration of p53 function leads to tumour regression *in vivo*. *Nature* **445**, 661–665 (2007).
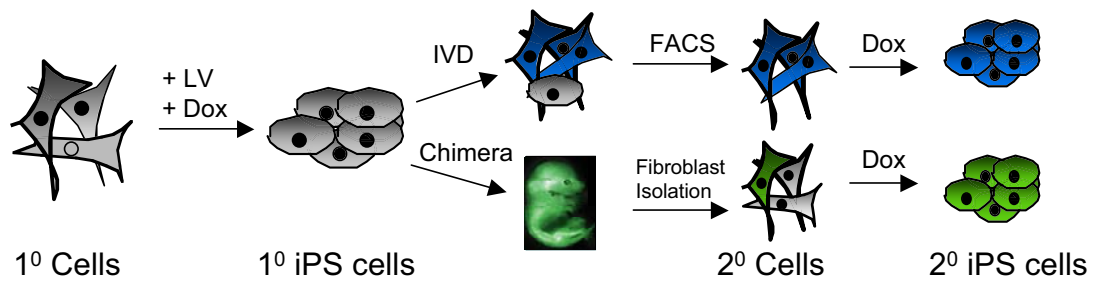
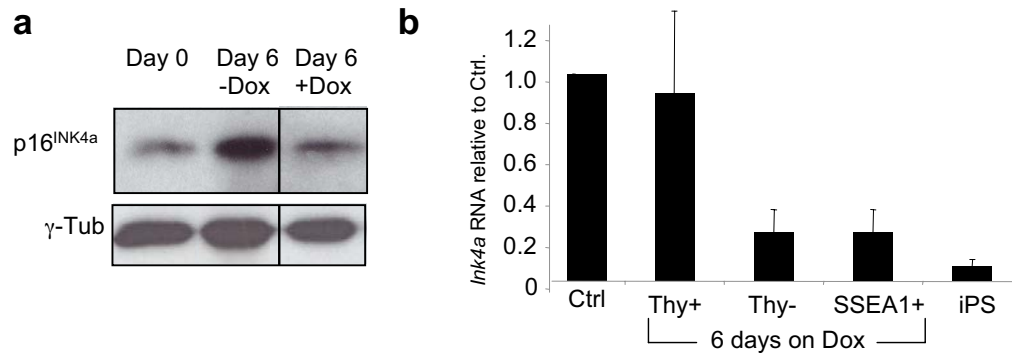**Supplementary Figure 1. Scheme of secondary (2°) cell generation from iPS cells**. Primary (1°) cells were infected with polycistronic lentivirus (LV) in the presence of doxycycline (Dox) to produce 1° iPS cells, which were either in vitro differentiated (IVD) into $Thy1^+$, $Flk1^+$, $SSEA1^-$ fibroblast-like 2° cells, or labeled with lentivirus constitutively expressing GFP and injected into blastocysts to recover 2° murine embryonic fibroblasts (MEFs) at E14.5.

a

b
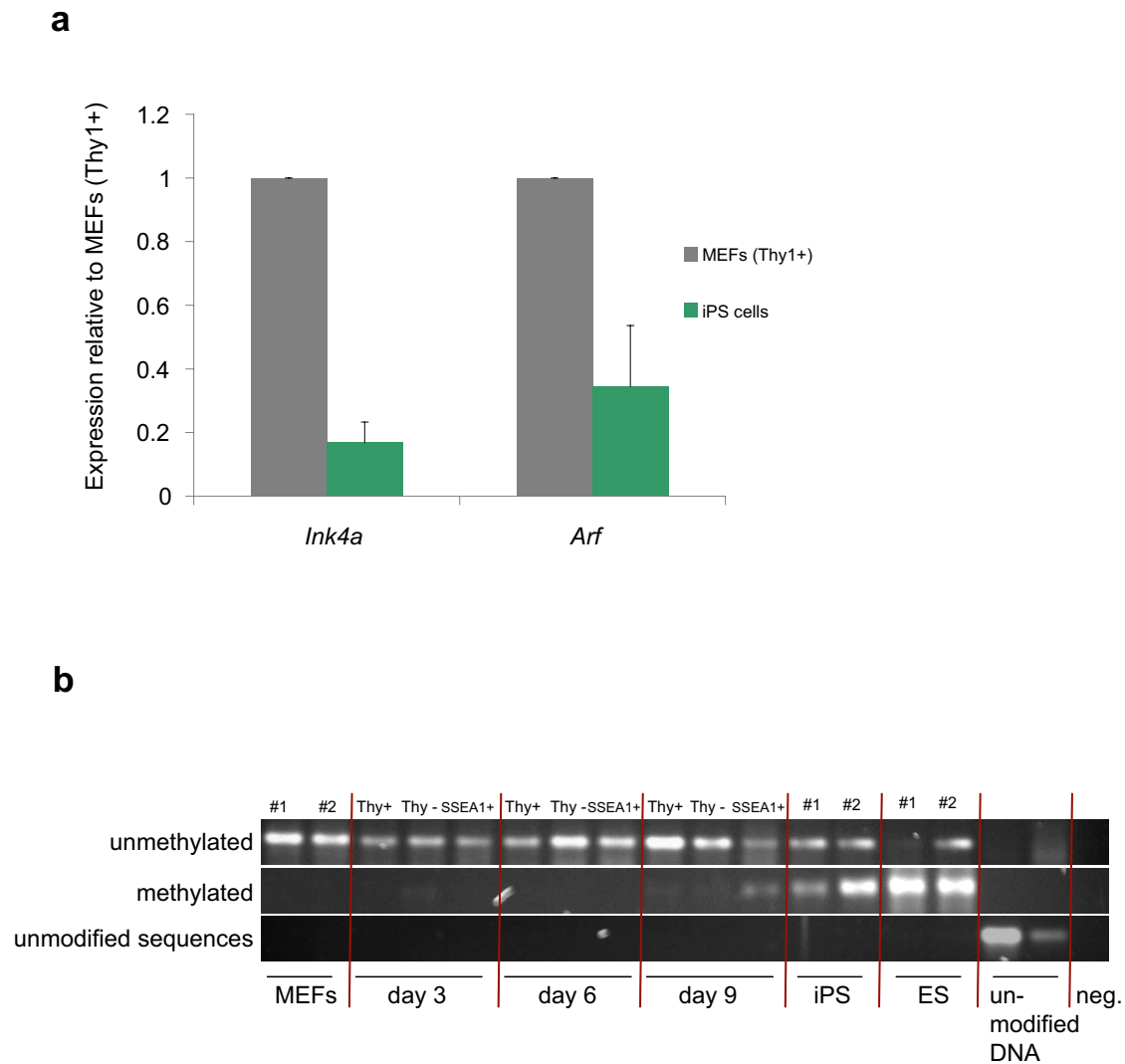
Supplementary Figure 2. Silencing of the *Ink4a/Arf* locus in iPS cells.

(a) RT-qPCR for *Ink4a* and *Arf* in MEFs and derivative iPS cells. Note the low expression levels of of both genes in iPS cells compared to MEFs. **(b)** Methylation specific PCR of the *Ink4a/Arf* locus in MEFs, intermediate cell populations, iPS cells and ES cells. Note that methylation of the locus occurs only in the SSEA1^{+} intermediates isolated at day 9 and remains methylated in iPS cells. Control ES cells also show strong methylation of the locus.

Supplementary Figure 3. Downregulation of *Ink4a* expression during reprogramming.

(a) Downregulation of p16[Ink4a] in bulk population of secondary MEFs exposed to doxycycline for 6 days, as determined by Western blot analysis. **(b)** Downregulation of *Ink4a* transcript in Thy1^{-} and SSEA1^{+} subpopulations after 6 days of transgene expression

a

b

c

d

e

f
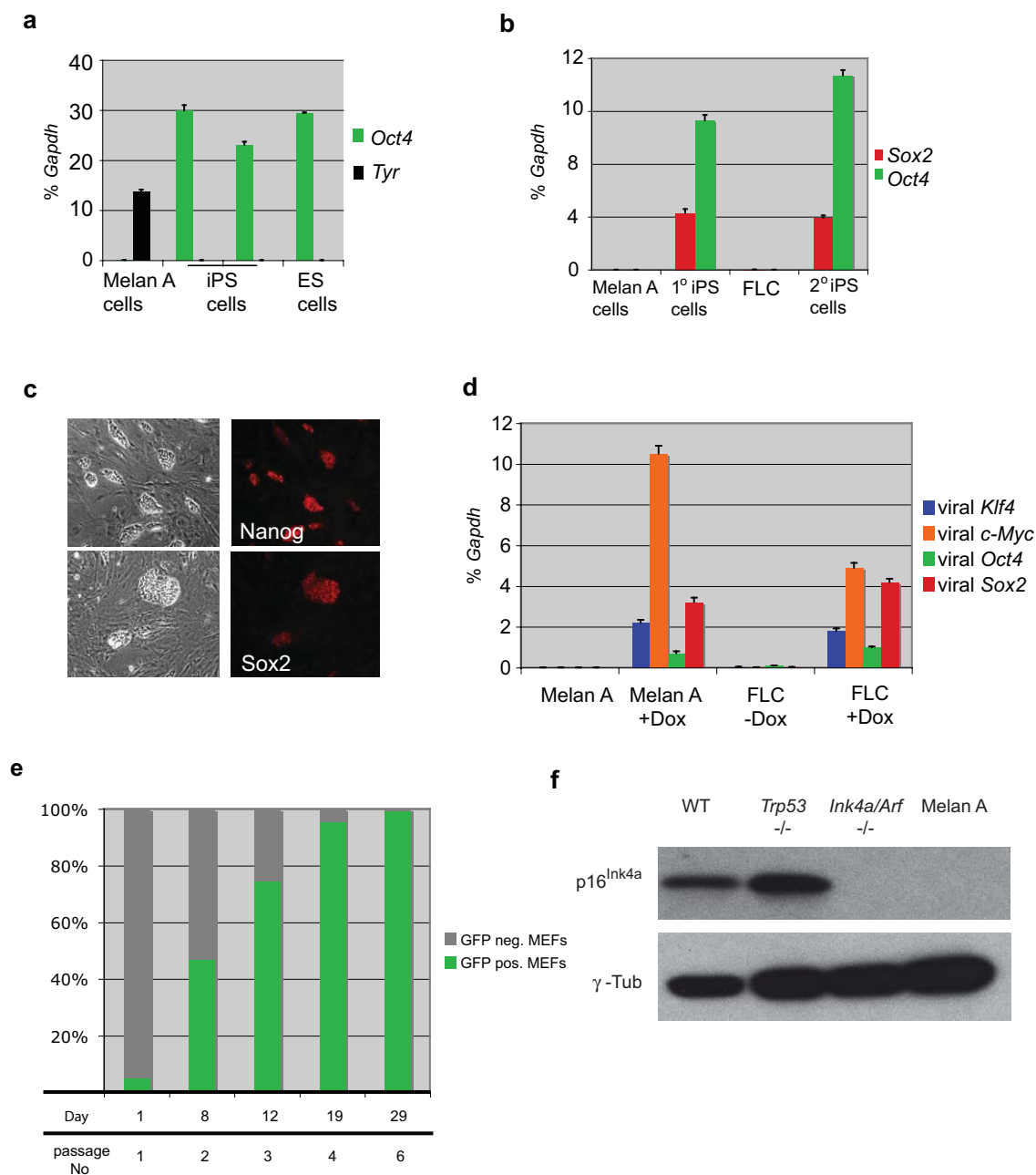
Supplementary Figure 4. Molecular and functional characterization of Melan A-derived secondary cells.

(a) qPCR for the melanocyte marker tyrosinase (Tyr) and the pluripotency marker *Oct4* in Melan A cells, two independently derived iPS cell clones and control ES cells. ND = not detected. **(b)** qPCR for *Oct4* and *Sox2* in Melan A cells, primary iPS cells, fibroblast-like secondary cells (FLC) and resultant secondary iPS cells. Note the absence of pluripotency markers in somatic cells and their activation upon conversion into iPS cells. **(c)** Immunofluorescence images for Nanog and Oct4 of iPS colonies derived from Melan A cells. **(d)** qPCR for viral transgene expression in directly infected Melan A cells and

secondary FLC in the presence of doxycycline. Note the absence of transgene expression in the absence of doxycycline induction. **(e)** Growth behavior of GFP[+] (iPS cell-derived) and GFP[-] (host blastocyst-derived) MEFs was determined by flow cytometry at different passages until day 29. Note the selective growth advantage of GFP[+] over GFP[-] MEFs over time, reflecting their immortality. **(f)** Western blot analysis for p16[Ink4a] in wild type (WT) fibroblasts, *Trp53-/-* fibroblasts, *Ink4a/Arf-/-* fibroblasts and Melan A cells (γ-tubulin was used as loading control).

a


b

Endoderm   Ectoderm   Mesoderm
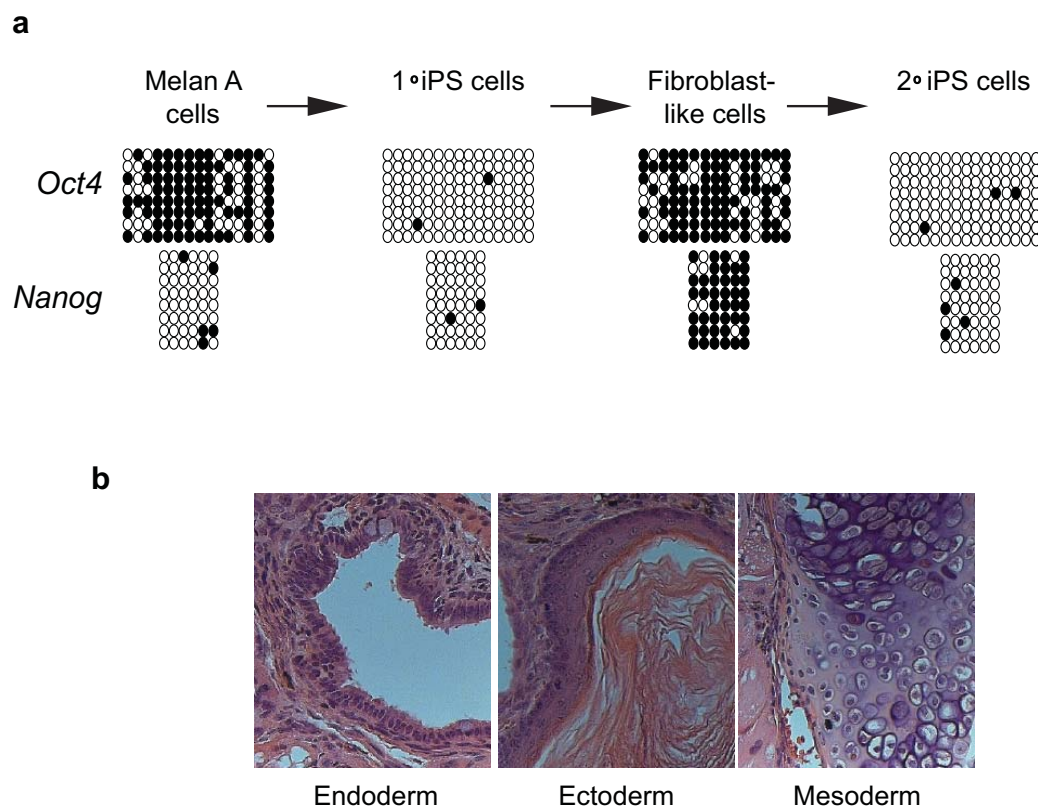
Supplementary Figure 5. Promoter methylation and developmental potential in Melan A-derived cells.

(a) Methylation status of the *Oct4* and *Nanog* promoters in the indicated cell populations as assessed by bisulfite sequencing. Black circles represent methylated cytosines while open circles represent unmethylated cytosines. **(b)** Hematoxylin and Eosin stained teratoma section produced from secondary Melan A- derived iPS cell clone. Note differentiation into structures indicative of ectodermal (keratinized epithelium), endodermal (glandular structures) and mesodermal (cartilage) tissues.
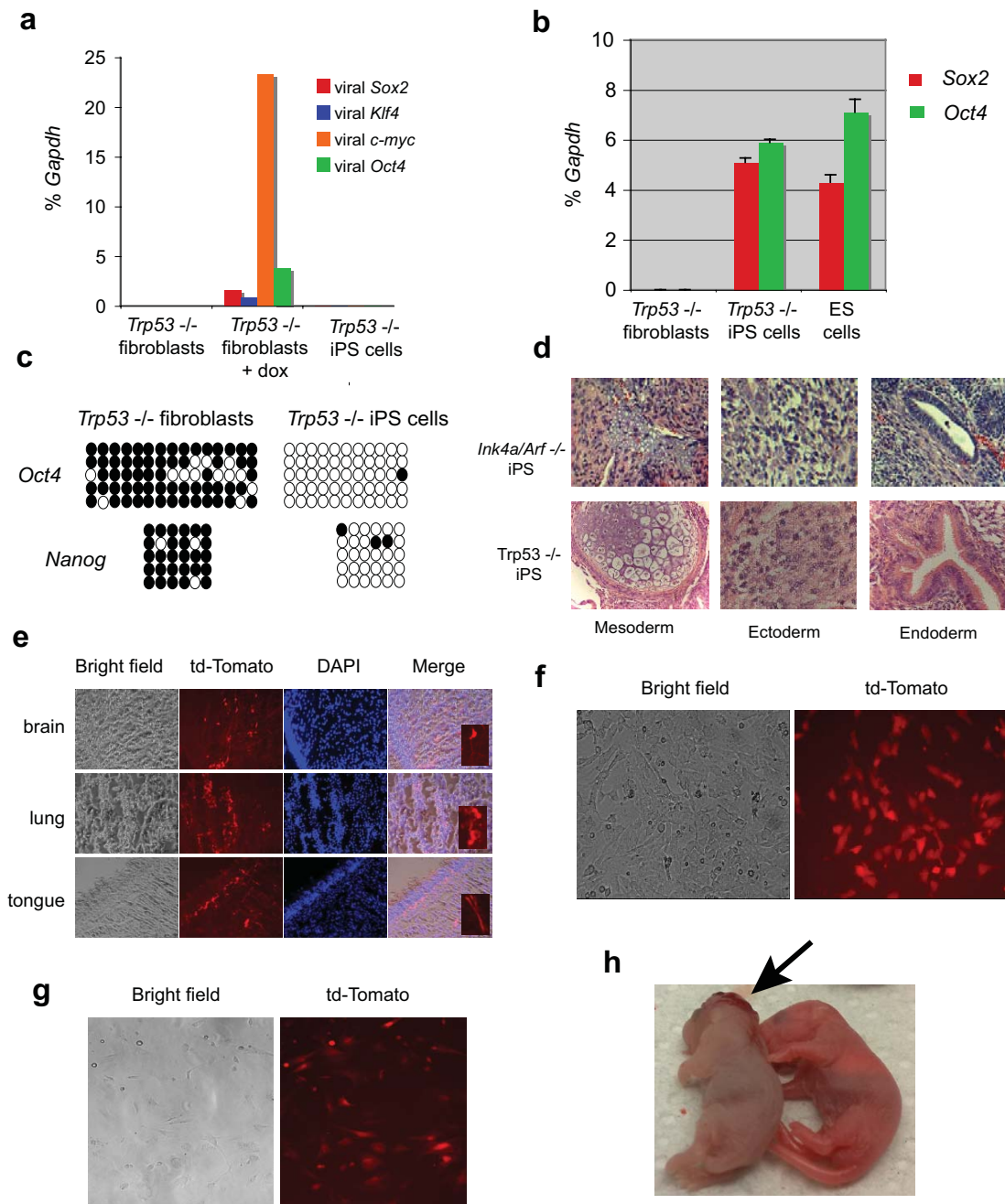
Supplementary Figure 6. Molecular and functional characterization of *Trp53* and *Ink4a/Arf*-deficient iPS cells.

(a) qPCR for viral transgene expression in untreated *Trp53*-/- fibroblasts, virally infected fibroblasts in the presence of doxycycline and derivative stable iPS cells upon discontinuation of doxycycline. **(b)** qPCR for endogenous *Oct4* and *Sox2* indicates expression of these markers in *Trp53*-/- iPS cells at levels comparable to WT ES cells. **(c)** Bisulfite methylation analysis of *Oct4* and *Nanog* promoters in *Trp53*-/- fibroblasts and derivative iPS cells. Note promoter demethylation in iPS cells. **(d)** Differentiation potential of *Trp53*- and *Ink4a/Arf*-deficient iPS cells as assessed by teratoma formation. Shown are typical endodermal, mesodermal and ectodermal structures. **(e)** Immunofluorescence for tdTomato of a newborn chimeric pup produced with *Trp53*-/- iPS cells that have been labeled with a lentivirus constitutively expressing tdTomato. Note contribution of iPS cells to different tissues (brain, lung, tongue). **(f)** tdTomato+ MEFs isolated from *Trp53*-/- iPS cell-derived E13.5 chimera. **(g)** tdTomato+ MEFs

a

b

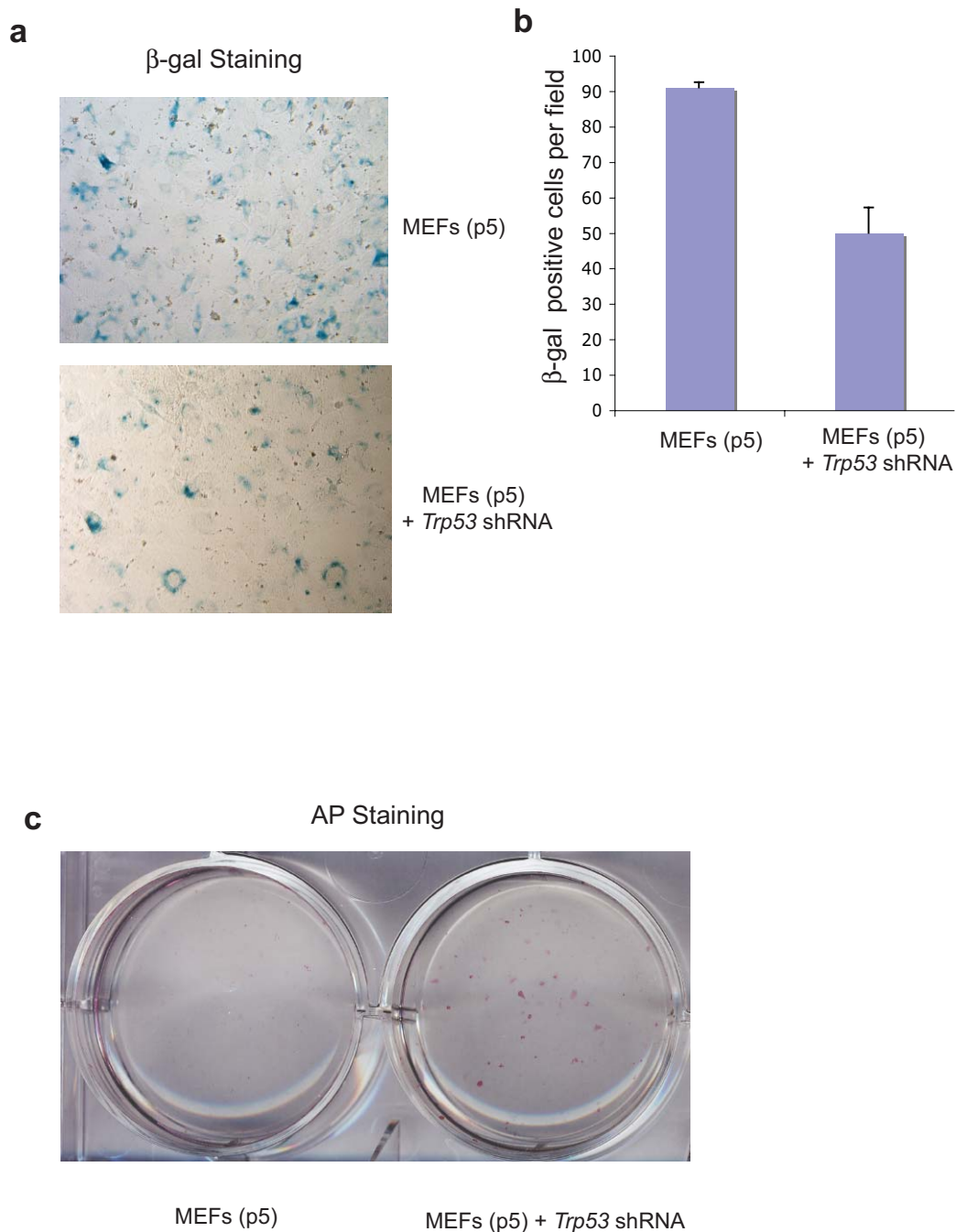AP staining

WT 15% FBS   *Trp53* -/- 15% FBS

c
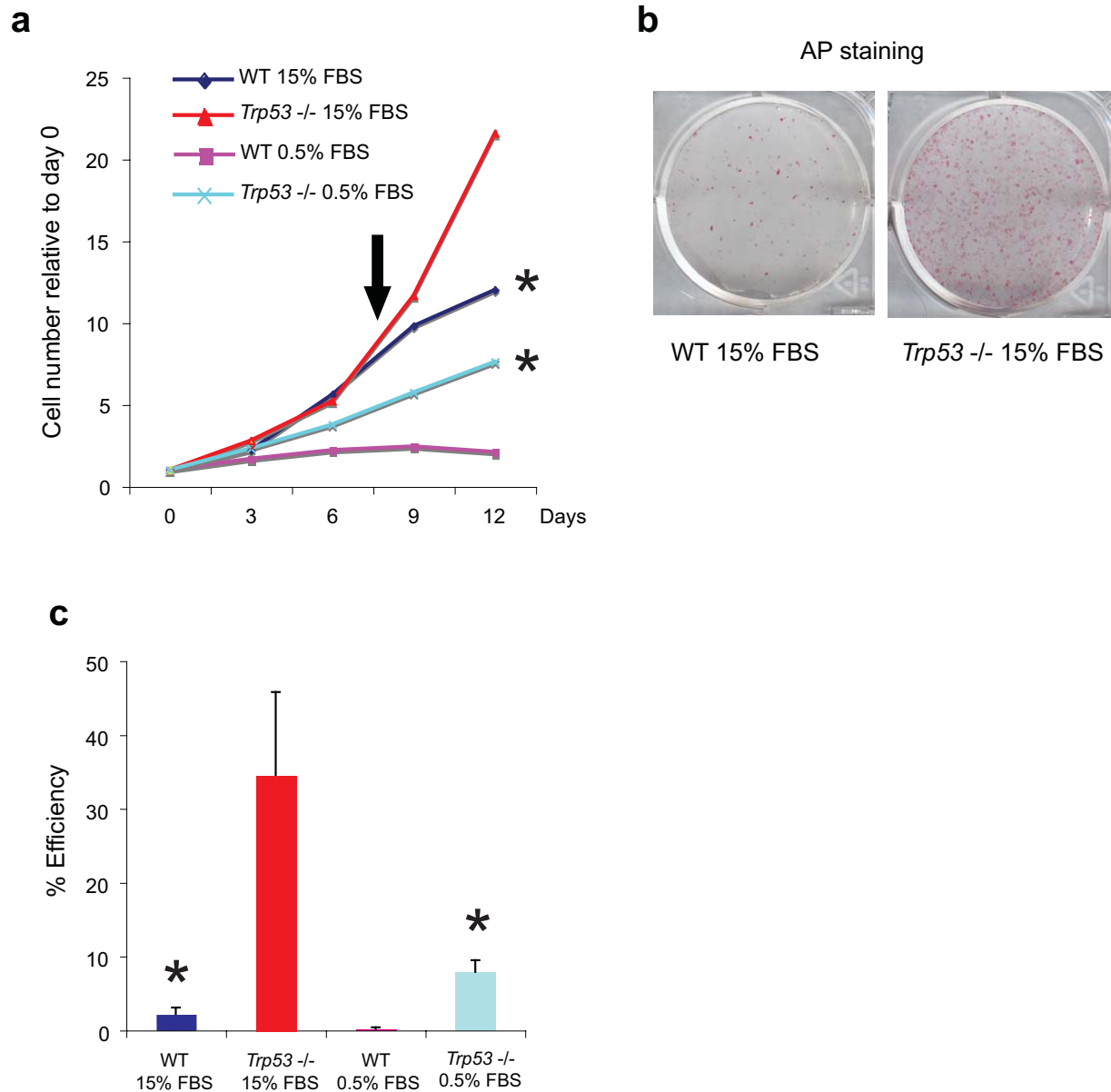
Supplementary Figure 7. Enhanced reprogramming potential of immortal cells depends on long-term growth potential, not actual growth rate.

(a) Growth curves of WT and *Trp53*-/- MEFs cultured in either low (0.5%) or high (15%) serum. **(b)** AP staining of iPS cell colonies derived from 4-factor-infected WT and *Trp53*-/- MEFs induced with doxycyline for 8 days, when growth rates are still comparable in 15% FBS (black arrow in (a)); colonies were scored on day 13 to ensure transgene-independence of colonies. Note that WT and *Trp53*-/- MEFs show different reprogramming potentials despite similar growth rates. **(c)** Reprogramming efficiencies of *Trp53*-/- and WT MEFs cultured in low and high serum. Note increased reprogramming potential of *Trp53*-/- MEFs grown at 0.5% serum over WT cells grown at 15% (relevant bars marked by asterisks) despite higher growth rate of WT cells over *Trp53*-/- cells (see curves in (a), marked by asterisks).
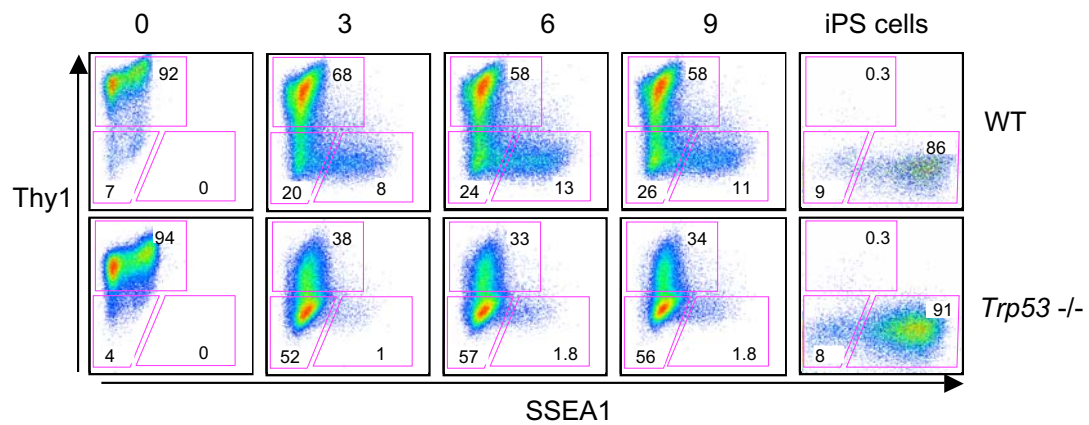
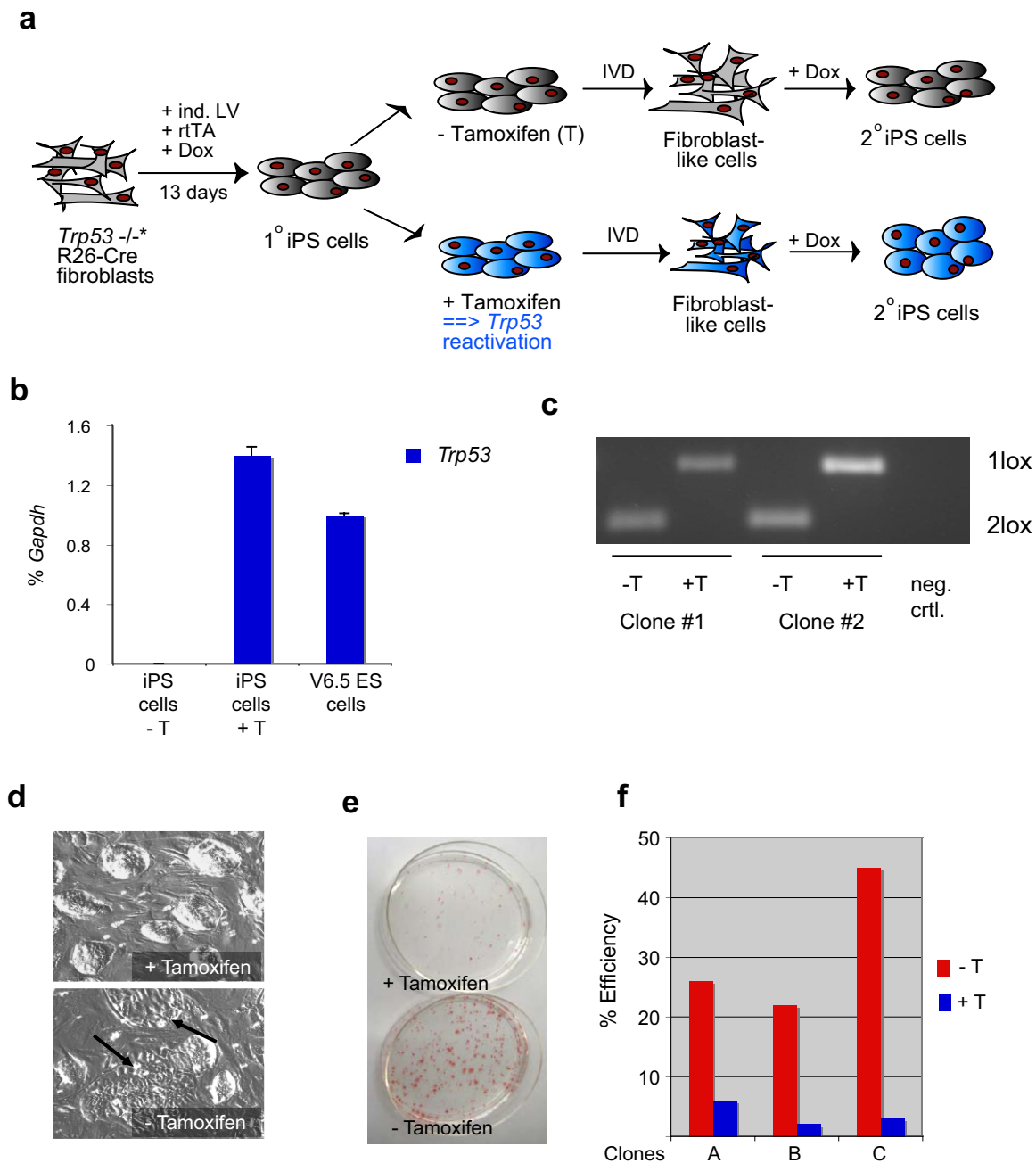**Supplementary Figure 8. Reprogramming kinetics of WT and *Trp53*-/- cells.**
FACS analysis for Thy1^{+} and SSEA1^{+} subpopulations appearing in WT and *Trp53*-/-
secondary MEFS at days 0, 3, 6 and 9 after transgene expression.

a

β-gal Staining

MEFs (p5)

MEFs (p5)
+ *Trp53* shRNA

b

c

AP Staining

MEFs (p5)   MEFs (p5) + *Trp53* shRNA

Supplementary Figure 9. Acute inactivation of *Trp53* endows senescent cultures with reprogramming potential.

(a) Shown are secondary MEFs at passage 5 stained for senescence-associated β-galactosidase in the presence of *Trp53* shRNA or a control vector. **(b)** Quantification of β-galactosidase positive cells. **(c)** AP staining of iPS cell-like colonies emerging from control vector or *Trp53* shRNA-infected secondary cells. Note that senescent cultures treated with *Trp53* shRNA can overcome the reprogramming block to generate iPS cell colonies. AP staining was performed 5 days after withdrawal of doxycycline from cultures to ensure transgene-independent self-renewal.

Supplementary Figure 10. Continuous *Trp53* deficiency is required for enhanced reprogramming efficiency.

(a) Schematic representation of *Trp53* reactivation experiment. Tail-tip fibroblasts from a mouse carrying a conditionally reactivatable *Trp53* allele (designated "-*" allele) and a constitutive null allele (designated "-" allele) as well as a *ROSA26* promoter driven tamoxifen-inducible CreER allele were infected with the four doxycycline-inducible lentiviruses to produce primary iPS cells. Treatment of iPS cell clones with tamoxifen resulted in the reactivation of one *Trp53* allele (designated "+" allele). Subsequent in vitro differentiation (IVD) yielded secondary cells, which converted into secondary iPS cells upon treatment with doxycycline. **(b)** qPCR for *Trp53* transcripts in untreated (-T)

cassette, which indicates reactivation of the wild type *Trp53* allele while 2lox denotes non-excised non-functional allele. **(d)** Representative colonies of *Trp53-/-** iPS cell colonies before and after tamoxifen treatment. Note the disappearance of differentiated colonies upon reactivation of *Trp53*. This is likely due to the loss of iPS cell-derived differentiated cells that had a growth advanatge in the absence of *Trp53*. **(e)** AP staining of plates seeded with secondary cells from tamoxifen-treated (*Trp53+/-*) or untreated (*Trp53-/-*) iPS cells. **(f)** Reprogramming efficiencies of secondary cells derived from tamoxifen-treated (*Trp53+/-*) or untreated (*Trp53-/-*) iPS cells.
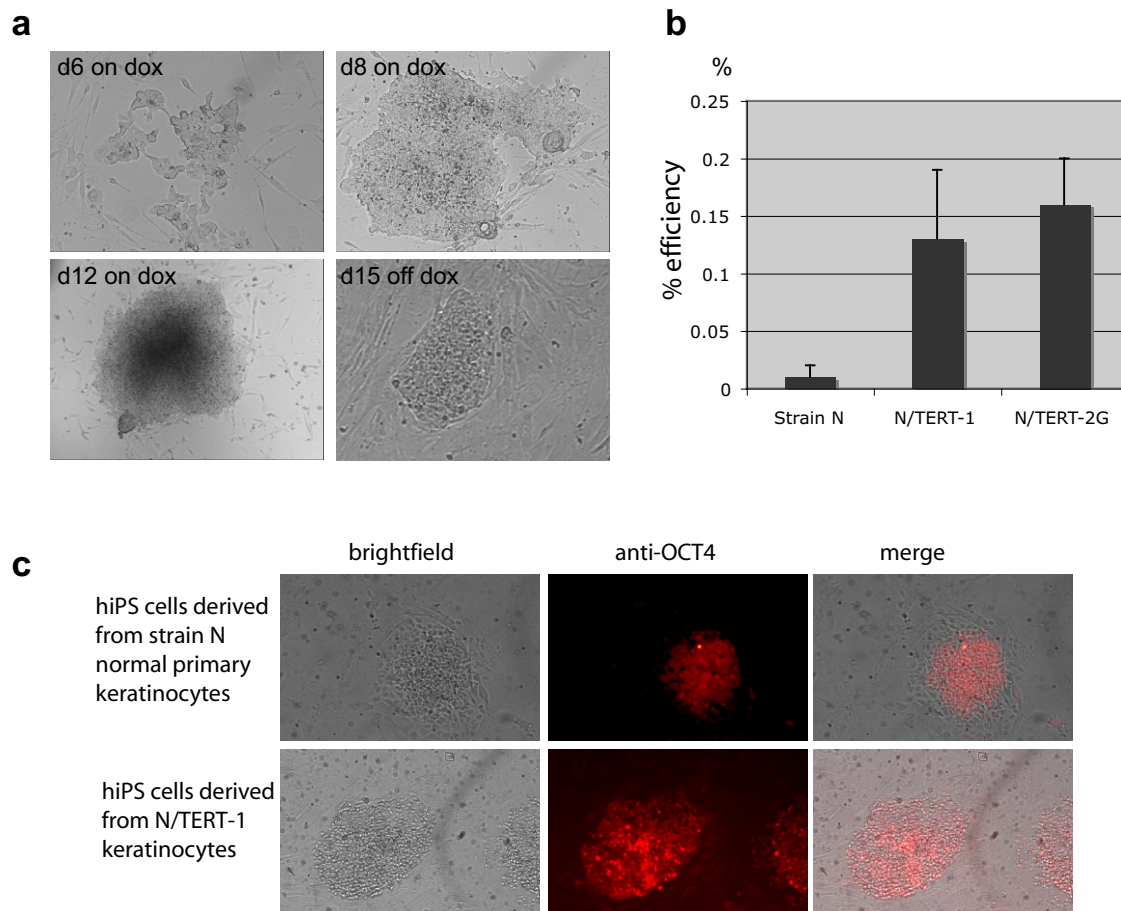
Supplementary Figure 11. TERT-immortalized human keratinocytes yield more iPS-like colonies than primary keratinocytes.

(a) N/TERT immortalized keratinocytes cell line (N/TERT-1) was co-infected with a polysistronic doxycycline-inducible lentivirus and a lentivirus constitutively expressing rtTA and the appearance of colonies was followed over time. **(b)** Reprogramming efficiencies of two different N/TERT immortalized keratinocyte cell lines (N/TERT-1 and N/TERT2G) compared with strain N primary normal keratinocytes. **(c)** Immunofluorescence for OCT4 in iPS-like colonies derived from WT keratinocytes and N/TERT immortalized keratinocytes cell line (N/TERT-1) following withdrawal of doxycycline.

Supplementary Table 1: Karyotypes of varius iPS cell lines.

Nomenclature	Cells	Results
11p5subclone	Melan A cells	Trisomy 6 plus randon chromosome gain and loss.
9p3	Melan A iPS 57	Very heterogenous and unstable with various abnormalities.
10p3	Melan A iPS 59	Half hyperdiploid, half hypertetraploid (near octoploid). Trisomy 6 and 8.
12p10	p53 -/-	All cells polyploid with ~80% tetraploid. Loss of 1 plus other abnormalities.
1p4	p53 -/- iPS #1	Hypotetraploid (66-73). Balanced 4/Y translocation
3p4	p53 -/- iPS #2	Tetraploid (72-80 chrom.). Same 4/Y translocation as 1p4.
5p4	p53 -/- iPS #3	Diploid (40-42). Unstable. Same 4/Y translocation as 1p4.
2p4	p53 -/- iPS #1+ Tamoxifen	36% with unstabled hypertetraploid karyotype. Same 4/Y translocation as 1p4.
4p4	p53 -/- iPS #2+ Tamoxifen	Hypotetraploid (68-75)). Balanced 4/Y translocation. Very similar to 1p4
6p4	p53 -/- iPS #3+ Tamoxifen	Tetraploid (70-75 chrom.). Same 4/Y translocation as 1p4, plus others.
13p10	INK4A/ARF MEF	>90% polyploid plus other abnormalities. Both male and female clone present.
7p3	INK4A/ARF iPS #1	2 clones. Fewer abnormalities than 1-6. X loss, extra material in C3, deletion in X.
8p3	INK4A/ARF iPS #2	3 clones, all with distinct abnormalities (loss of X, gain of 8). Similar to 7p3.

Supplementary Table 2: primer sequences used for PCR analysis

Gene	Forward primer (5' to 3')	Reverse primer (5' to 3')
Gapdh	AGGTCGGTGTGAACGGATTTG	TGTAGACCATGTAGTTGAGGTCA
Dopachrome Tautomerase	CTAACCGCAGAGCAACTTGG	CAAGAGCAAGACGAAAGCTCC
Nanog	TTGCTTACAAGGGTCTGCTACT	ACTGGTAGAAGAATCAGGGCT
Tyrosinase	AGTTTACCCAGAAGCCAATGC	CGACTGGCCTTGTTCCAAGT
Klf4 (endogenous)	AACATGCCCGGACTTACAAA	TTCAAGGGAATCCTGGTCTTC
c-Myc (endogenous)	TAACTCGAGGAGGAGCTGGA	GCCAAGGTTGTGAGGTTAGG
Oct4 (endogenous)	TAGGTGAGCCGTCTTTCCAC	GCTTAGCCAGGTTCGAGGAT
Sox2 (endogenous)	TTAACGCAAAAACCGTGATG	GAAGCGCCTAACGTACCACT
c-Myc (lentiviral)	AAGAGGACTTGTTGCGGAAA	TTGTAATCCAGAGGTTGATTATCG
Klf4 (lentiviral)	ATGGTCAAGTTCCCAGCAAG	TGATATCGAATTCCGTTTGTTT
Oct4 (lentiviral)	GCTCGTTTAGTGAACCGTCAG	CGAAGTCTGAAGCCAGGTGT
Sox2 (lentiviral)	GGCCATTAACGGCACACT	AAGCAGCGTATCCACATAGC
p21	TTGCACTCTGGTGTCTGAGC	TGCGCTTGGAGTGATAGAAA
Ink4a	GTGTGCATGACGTGCGGG	GCAGTTCGAATCTGCACCGTAG
Arf	GCTCTGGCTTTCGTGAACATG	TCGAATCTGCACCGTAGTTGAG

Viral vectors and production

The generation and structure of replication-defective doxycycline-inducible lentiviral vectors and a lentiviral vector constitutively expressing the reverse tetracycline-controlled transactivator (rtTA) has been described in detail elsewhere[13, 28]. Viral supernatant was concentrated approximately 100-fold by ultracentrifugation at 50,000g for 1.5 h at 4 °C, resuspended in 300 μl PBS, and stored at -80 °C. Infections were carried out in 1 ml medium using 5 μl of each viral concentrate per 35-mm plate. Downregulation of Trp53 expression was performed by infecting cells with a lentiviral construct expressing an shRNA against *Trp53* (GTACTCTCCTCCCCTCAAT) as previously described[20].

Cell culture and *in vitro* differentiation of iPS cells

Melan A cells were grown in RPMI medium containing 10% FCS and 200 nM 12-*O*-tetradecanoylphorbol-13-acetate (TPA)[17]. Melan A cells were single-cell cloned and only one subclone was used for subsequent experiments. Fibroblast cultures containing a reactivatable *Trp53* allele as well as the ROSA26-CreER allele[29] were obtained from the tail of an adult mouse as described previously[13]. *Trp53*$^{-/-}$ fibroblasts and *Ink4a/Arf*$^{-/-}$ MEFs were cultured in DMEM containing 10% FCS. Primary melanocytes were purchased from the Skin Diseases Research Center, Yale School of Medicine, and were grown like Melan A cells. For lentiviral vector infections, cells were seeded in 6-well plates at a density of 1 x 10^5 cells per well and infected on three consecutive days. Medium changes were performed 12–24 h after infection. One day after the last infection, ES cell medium containing 1 μg ml^{-1} doxycycline was added. Fresh ES cell medium with doxycycline was added every other day until iPS cell colonies developed. Five days later, cell culture conditions were switched to ES cell medium in the absence of doxycycline. iPS cell colonies were picked into 96-well plates containing PBS without magnesium and calcium using a 10 μl pipette. Trypsin was added to each well, incubated for 5 min and single-cell suspension was transferred into 24-well dishes containing MEF feeder layers. Picked iPS cells were grown on MEFs in standard ES cell conditions. For blastocyst injections, iPS cells were marked with a FUGW lentiviral vector constitutively expressing GFP. For *in vitro* differentiation assays, iPS cells were grown in the absence of leukaemia inhibitory factor (LIF) on uncoated plates to induce embryoid body formation. Embryoid bodies were explanted on gelatinized plates and outgrowths were dissociated by trypsinization and expanded for FACS purification (see flow cytometry).

Human cell culture and generation of human iPS cells

The human epidermal keratinocyte lines strain N, N/TERT-1, and N/TERT-2G were grown in keratinocyte serum-free medium (KSFM) medium as previously described[21]. STEMCCA lentiviral vector[28] infections were carried out with human keratinocytes in 6-well plates at a density of 100,000 cells per well on two subsequent days. The infection efficiency of primary human keratinocytes after two subsequent infections with tetO-GFP lentiviral vector in the presence of the rtTA expressing lentiviral vector was 40%. Medium changes were performed 12 h after infections, and 1 day after infection human keratinocytes were transferred to MEFs. Media containing 50% keratinocyte medium and 50% human ES cell medium containing 0.5 μg ml^{-1} doxycycline was added 1 day later. Medium changes were performed every other day in the presence of 0.5 μg ml^{-1} doxycycline until colonies developed. After the appearance of human ES-cell-like colonies, medium was switched to human ES cell culture conditions and human iPS cells were picked and further expanded as described previously[8].

Calculation of reprogramming efficiencies

For cells directly infected with lentivirus (LV-tetO-Oct4, -Sox2, -Klf4 and -c-Myc[13] plus FUGW-rtTA[13], or LV-tetO-STEMCCA[28] plus FUGW-rtTA), reprogramming efficiencies were calculated on the basis of the infection efficiency of somatic cells with a single control virus expressing EGFP (FUGW-GFP) or by performing immunofluorescence staining for Oct4 and Sox2. For secondary cells, equal numbers of cells were plated in the absence or presence of doxycycline on 100-mm dishes coated with gelatin or containing a layer of irradiated

MEF feeders. Efficiencies were determined on average 20 days later by dividing the number of iPS cell colonies that grew after the withdrawal of doxycycline by the number of seeded cells, or alternatively, by the number of colonies that adhered to the control plate in the absence of doxycycline. ES cell character of iPS cell colonies was validated by immunofluorescence staining for Nanog. For some experiments, we FACS-sorted single secondary cells (previously marked with a lentiviral vector expressing td-Tomato) into wells of a 96-well plate. Reprograming was induced by treatment of cells with doxycycline for 15 days, followed by doxycycline-independent growth for another 7 days. The number of wells with ES cell-like transgene-independent colonies was then scored by morphology and alkaline phosphatase staining; ES cell phenotype of these colonies was further verified by immunofluorescence staining for Nanog and Sox2. Efficiencies were calculated on the basis of the number of wells containing colonies, normalized by the seeding efficiency, which was determined at day 3 by the presence of at least one td-Tomato cell in the well.

Alkaline phosphatase staining

Alkaline phosphatase staining was performed using an Alkaline Phosphatase substrate kit (Vector laboratories) according to manufacturer's recommendations.

Immunofluorescence

iPS cells were cultured on pretreated coverslips, fixed with 4% PFA, and permeabilized with 0.5% Triton X-100. The cells were then stained with primary antibodies against mouse Oct4 (sc-8628, Santa Cruz), mouse Sox2 (AB5603, Chemicon), and mouse Nanog (ab21603, Abcam). Respective secondary antibodies were conjugated to Alexa Fluor 546 (Invitrogen). Nuclei were counterstained with 4,6-diamidino-2-phenylindole (DAPI; Invitrogen). Cells were imaged with a Leica DMI4000B inverted fluorescence microscope equipped with a Leica DFC350FX camera. Images were processed and analysed with Adobe Photoshop software.

Flow cytometry

Collected cells were incubated with antibodies against Thy1.2 (phycoerythrin (PE)-conjugated, 53-2.1, eBiosciences), SSEA1 (mouse IgM, MC-480, Developmental Hybridoma Bank) and Flk1 (biotinylated, Aves 12a1, eBiosciences) for 20 min. Cells were washed in PBS and then incubated for 20 min with allophycocyanin (APC)-conjugated anti mouse IgM (eBioscience) and Pacific Blue-conjugated streptavidin (Invitrogen). The cells were washed in PBS, resuspended in propidium iodide 5% FBS/PBS solution, and passed through a 40-µm cell strainer to achieve single-cell suspension. Cells positive for Thy1 and Flk1 and negative for SSEA1 were sorted on a FACSAria (BD Biosciences). For analysis and/or sorting of intermediates, cells were stained with Thy1.2 and SSEA1 antibodies and sorted or analysed as indicated.

PCR analysis

For quantitative PCR (qPCR) analysis, RNA was isolated from cells with TRIzol reagent (Invitrogen). For strongly pigmented cells, an extra phenol–chloroform purification step was performed before RNA clean up with the RNeasy Minikit (Qiagen). Complementary DNA was produced with the Super Script III kit (Invitrogen). Real-time quantitative PCR reactions were set up in triplicate with the Brilliant II SYBR Green QPCR Master Mix (Stratagene), and run on a Mx3000P QPCR System (Stratagene). Primer sequences are listed in Supplementary Table 2. Genotyping for the *Trp53*^{-/-}* allele was performed by PCR using the following three primer pairs: P53K_A: 5'-CAAACTGTTCTACCTCAAGAGCC-3', P53K_B: 5'-AGCTAGCCACCATGGCTTGAGTAAGTCTGCA-3', and P53K_C: 5'-CTTGGAGACATAGCCACACTG-3' (provided by A. Ventura).

Western blot analysis

Cell extracts were run in 15% SDS–PAGE gels. The gels were run at 90 V until proteins were separated (~2 h) and transferred to PVDF membranes (Bio-Rad) by running overnight at 20 V, 4 °C in transfer apparatus (Bio-Rad). The membranes were washed in PBS-T (PBS + 0.1% Tween) and blocked in 5% milk in PBS-T for 1 h. The membranes were then incubated with anti-p16[Ink4A], anti-Trp53 (phospho s15) (abcam) and γ-tubulin

antibody overnight at 4 °C, washed and incubated in horseradish-peroxidase-conjugated anti-rabbit antibodies for 1 h at room temperature. Immunoblots were visualized using ECL reagent (Santa Cruz).

Cellular senescence detection

Cellular senescence was detected using a cellular senescence detection kit (Millipore) on the basis of β-galactosidase staining according to manufacturer's recommendations.

Bisulphite sequencing

Bisulphite treatment of DNA was performed with the EpiTect Bisulfite Kit (Qiagen) according to manufacturer's instructions. Primer sequences were as previously described for *Oct4* and *Nanog*[4]. Amplified products were purified by using gel filtration columns, cloned into the pCR4-TOPO vector (Invitrogen), and sequenced with M13 forward and reverse primers.

Generation of teratomas and chimaeras

For teratoma induction, 2 x 10^6 cells of each iPS cell line were injected subcutaneously into the dorsal flank of isoflurane-anaesthetized SCID mice. Teratomas were recovered 3–5 weeks after injection, fixed overnight in 10% formalin, paraffin embedded, and processed with haematoxylin and eosin. For chimaera production, female BDF1 mice were superovulated with PMS (pregnant mare serum) and hCG (human chorion gonadotropin) and mated to BDF1 stud males. Zygotes were isolated from plugged females 24 h after hCG injection. After 3 days of *in vitro* culture in KSOM media, blastocysts were injected with iPS cells, and transferred into day 2.5 pseudopregnant recipient females. Caesarean sections were performed 17 days later and pups were fostered with lactating females.

1. • Hochedlinger, K. & Plath, K. Epigenetic reprogramming and induced pluripotency. Development 136, 509–523 (2009) | Article | PubMed | ChemPort |
2. • Takahashi, K. *et al.* Induction of pluripotent stem cells from adult human fibroblasts by defined factors. Cell 131, 861–872 (2007) | Article | PubMed | ChemPort |
3. • Takahashi, K. & Yamanaka, S. Induction of pluripotent stem cells from mouse embryonic and adult fibroblast cultures by defined factors. Cell 126, 663–676 (2006) | Article | PubMed | ISI | ChemPort |
4. • Maherali, N. *et al.* Directly reprogrammed fibroblasts show global epigenetic remodeling and widespread tissue contribution. Cell Stem Cell 1, 55–70 (2007) | Article | PubMed | ChemPort |
5. • Okita, K., Ichisaka, T. & Yamanaka, S. Generation of germline-competent induced pluripotent stem cells. Nature 448, 313–317 (2007) | Article | PubMed | ISI | ChemPort |
6. • Wernig, M. *et al. In vitro* reprogramming of fibroblasts into a pluripotent ES-cell-like state. Nature 448, 318–324 (2007) | Article | PubMed | ISI | ChemPort |
7. • Hockemeyer, D. *et al.* A drug-inducible system for direct reprogramming of human somatic cells to pluripotency. Cell Stem Cell 3, 346–353 (2008) | Article | PubMed | ChemPort |
8. • Maherali, N. *et al.* A high-efficiency system for the generation and study of human induced pluripotent stem cells. Cell Stem Cell 3, 340–345 (2008) | Article | PubMed | ChemPort |
9. • Wernig, M. *et al.* A drug-inducible transgenic system for direct reprogramming of multiple somatic cell types. Nature Biotechnol. 26, 916–924 (2008) | Article
10. • Collado, M., Blasco, M. A. & Serrano, M. Cellular senescence in cancer and aging. Cell 130, 223–233 (2007) | Article | PubMed | ISI | ChemPort |
11. • Parrinello, S. *et al.* Oxygen sensitivity severely limits the replicative lifespan of murine fibroblasts. Nature Cell Biol. 5, 741–747 (2003) | Article
12. • Zindy, F. *et al.* Arf tumor suppressor promoter monitors latent oncogenic signals *in vivo*. Proc. Natl Acad. Sci. USA 100, 15930–15935 (2003) | Article | PubMed | ChemPort |

13. • Stadtfeld, M., Maherali, N., Breault, D. T. & Hochedlinger, K. Defining molecular cornerstones during fibroblast to iPS cell reprogramming in mouse. Cell Stem Cell 2, 230–240 (2008) | Article | PubMed | ChemPort |

14. • Brambrink, T. *et al.* Sequential expression of pluripotency markers during direct reprogramming of mouse somatic cells. Cell Stem Cell 2, 151–159 (2008) | Article | PubMed | ChemPort |

15. • Sharpless, N. E. *et al.* Loss of p16Ink4a with retention of p19Arf predisposes mice to tumorigenesis. Nature 413, 86–91 (2001) | Article | PubMed | ISI | ChemPort |

16. • Serrano, M. *et al.* Role of the INK4a locus in tumor suppression and cell mortality. Cell 85, 27–37 (1996) | Article | PubMed | ISI | ChemPort |

17. • Bennett, D. C., Cooper, P. J. & Hart, I. R. A line of non-tumorigenic mouse melanocytes, syngeneic with the B16 melanoma and requiring a tumour promoter for growth. Int. J. Cancer 39, 414–418 (1987) | Article | PubMed | ISI | ChemPort |

18. • Kamijo, T. *et al.* Tumor suppression at the mouse INK4a locus mediated by the alternative reading frame product p19ARF. Cell 91, 649–659 (1997) | Article | PubMed | ISI | ChemPort |

19. • Hanna, J. *et al.* Direct reprogramming of terminally differentiated mature B lymphocytes to pluripotency. Cell 133, 250–264 (2008) | Article | PubMed | ChemPort |

20. • Ventura, A. *et al.* Cre-lox-regulated conditional RNA interference from transgenes. Proc. Natl Acad. Sci. USA 101, 10380–10385 (2004) | Article | PubMed | ChemPort |

21. • Dickson, M. A. *et al.* Human keratinocytes that express hTERT and also bypass a p16(INK4a)-enforced mechanism that limits life span become immortal yet retain normal growth and differentiation characteristics. Mol. Cell. Biol. 20, 1436–1447 (2000) | Article | PubMed | ISI | ChemPort |

22. • Mali, P. *et al.* Improved efficiency and pace of generating induced pluripotent stem cells from human adult and fetal fibroblasts. Stem Cells 26, 1998–2005 (2008) | Article | PubMed | ChemPort |

23. • Zhao, Y. *et al.* Two supporting factors greatly improve the efficiency of human iPSC generation. Cell Stem Cell 3, 475–479 (2008) | Article | PubMed | ChemPort |

24. • Molofsky, A. V. *et al.* Increasing p16INK4a expression decreases forebrain progenitors and neurogenesis during ageing. Nature 443, 448–452 (2006) | Article | PubMed | ISI | ChemPort |

25. • Krishnamurthy, J. *et al.* p16INK4a induces an age-dependent decline in islet regenerative potential. Nature 443, 453–457 (2006) | Article | PubMed | ISI | ChemPort |

26. • Janzen, V. *et al.* Stem-cell ageing modified by the cyclin-dependent kinase inhibitor p16INK4a. Nature 443, 421–426 (2006) | Article | PubMed | ISI | ChemPort |

27. • Eminli, S. *et al.* Differentiation stage determines reprogramming potential of hematopoietic cells into iPS cells. Nature Genet (in the press)

28. • Sommer, C. A. *et al.* iPS cell generation using a single lentiviral stem cell cassette. Stem Cells 27, 543–549 (2008) | Article | ChemPort |

29. • Ventura, A. *et al.* Restoration of p53 function leads to tumour regression *in vivo*. Nature 445, 661–665 (2007) | Article | PubMed | ISI | ChemPort |